

A compact ultrahigh-vacuum system for the *in situ* investigation of III/V semiconductor surfaces

Cite as: Review of Scientific Instruments **71**, 504 (2000); <https://doi.org/10.1063/1.1150232>

Submitted: 06 August 1999 . Accepted: 06 November 1999 . Published Online: 04 February 2000

Peter Geng, Juan Márquez, Lutz Geelhaar, et al.



View Online



Export Citation

ARTICLES YOU MAY BE INTERESTED IN

[A compact ultrahigh vacuum scanning tunneling microscope with dilution refrigeration](#)

Review of Scientific Instruments **89**, 113707 (2018); <https://doi.org/10.1063/1.5043636>



PFEIFFER VACUUM

Your Leak Detection Experts

The widest offer of leak testing solutions, using helium and hydrogen



Learn more!

A compact ultrahigh-vacuum system for the *in situ* investigation of III/V semiconductor surfaces

Peter Geng, Juan Márquez, Lutz Geelhaar, Jutta Platen, Carsten Setzer, and Karl Jacobi^{a)}

Fritz-Haber-Institut der Max-Planck-Gesellschaft, Faradayweg 4–6, D-14195 Berlin, Germany

(Received 6 August 1999; accepted for publication 6 November 1999)

A compact ultrahigh vacuum (UHV) system has been built to study growth and properties of III/V semiconductor surfaces and nanostructures. The system allows one to grow III/V semiconductor surfaces by molecular beam epitaxy (MBE) and analyze their surface by a variety of surface analysis techniques. The geometric structure is examined by scanning tunneling microscopy (STM), low-energy electron diffraction and reflection high-energy electron diffraction. The electronic properties of the surfaces are studied by angular resolved photoemission either in the laboratory using a helium discharge lamp or at the Berlin Synchrotron Radiation Facility BESSY. In order to meet the space restriction at BESSY the system dimensions are kept very small. A detailed description of the apparatus and the sample handling system is given. For the UHV-STM (Park Scientific Instruments, VP2) a new, versatile tip handling mechanism has been developed. It allows the transfer of tips out of the chamber and furthermore, the *in situ* tip cleaning by electron annealing. In addition, another more reliable *in situ* tip-preparation technique operating the STM in the field emission regime is described. The ability of the system is shown by an atomically resolved STM image of the $c(4\times 4)$ reconstructed GaAs(001) surface. © 2000 American Institute of Physics. [S0034-6748(00)04102-2]

I. INTRODUCTION

The growth of semiconductor nanostructures has attracted much interest due to their ability to provide low-dimensional electron confinement.^{1–4} Structures with one or zero dimensional electron confinement require the growth control on a lateral nanometer scale. Thus, the growth mechanism has to be studied at an atomic level. One of the most powerful techniques for such a purpose is scanning tunneling microscopy (STM) due to its imaging capability with atomic resolution. The key point is to link the STM to a molecular beam epitaxy chamber in order to investigate the grown layers *in situ*. For these reasons we have designed and built a compact multichamber UHV system, consisting of a III/V-semiconductor MBE facility linked to two independent UHV chambers which house a STM and further surface analytical tools.

II. SYSTEM DESCRIPTION

A schematic overview of the complete UHV apparatus is shown in Fig. 1. The system has been specially designed for experiments at the Berlin Synchrotron Radiation Facility [Berliner Elektronenspeicherring-Gesellschaft für Synchrotronstrahlung (BESSY)]. Two boundary conditions had to be considered: First, due to the limited space at the beamline, all elements of the system had to be aligned in the direction of the beamline. The dimensions of the apparatus are 2.4 m \times 0.9 m \times 1.8 m. Second, the transport of the apparatus

to and from BESSY demanded a construction as simple and stable as possible in order to avoid damages during the transportation.

Another very crucial point is sufficient vibrational damping for the STM. Our system is setup in the basement of the building and, moreover, it is mounted on an insulated concrete floor which is laid out on the natural sandy soil without any contact to the foundation walls. The samples are introduced into the chamber via the loading chamber (Fig. 1). This interlock part consists of a six-pass 2.75 in. cross, which is pumped independently by an ion-getter pump (Varian, Star Cell, 22 1s^{-1}). The downwards going tube of the cross houses a rack with four sample positions. After introducing samples into the vacuum system, the loading chamber has to be baked out ensuring that the samples are stored under UHV conditions and the transfer between MBE and STM chamber is in the UHV. Since we are able to introduce four samples each time, the bakeout does not occur very often. We had to renounce a fast entry chamber, because the space limitation at the BESSY beamline does not allow a more extended apparatus. Actually, the transfer line to the STM chamber, which is perpendicular to the chamber transfer line, as can be seen from Fig. 1, is not used at the synchrotron.

A. MBE chamber

The compact MBE growth chamber, shown schematically in Fig. 2, is equipped with three solid state evaporation Knudsen cells loaded with As, Ga, and In. The capacities of the crucibles are 250 cc for the As cell (DCA, Valved Cracker MBS-250-35-11 As) and 0.5 cc for the Ga/In cells (both Oxford Instruments, Miniature K-Cell), respectively.

^{a)}Author to whom correspondence should be addressed; electronic mail: jacobi@fhi-berlin.mpg.de

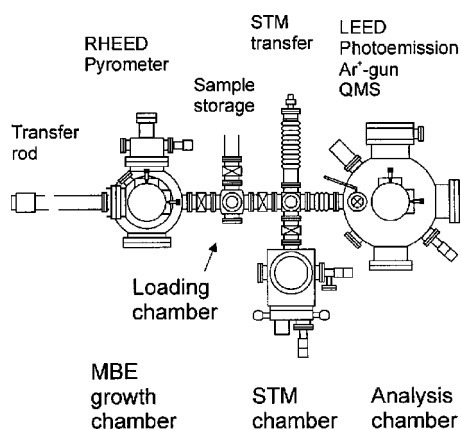


FIG. 1. Schematic top view of the vacuum system. Samples are introduced via the loading chamber, prepared in the MBE chamber and investigated *in situ* by STM or in the analysis chamber.

The sample is held facing downwards by a manipulator allowing motion in x , y , and z direction as well as 270° rotation about the axis normal to the sample surface. Sample heating is accomplished by thermal radiation from a filament which is mounted on the sample manipulator above the backside of the sample. The sample temperature is monitored with an IR-pyrometer (Kleiber, Pyroskop 202). Temperatures up to 620°C are reachable with this arrangement.

The growth rate and the surface quality during growth are monitored with a 3 kV reflection high energy electron diffraction system (RHEED). Epitaxial layers of 50–100 nm are typically grown at growth rates between 0.1 and 1.5 \AA s^{-1} . The pressure produced by the evaporation cells at the sample position (beam equivalent pressure) is measured with a movable ion gauge. This is placed above the RHEED elec-

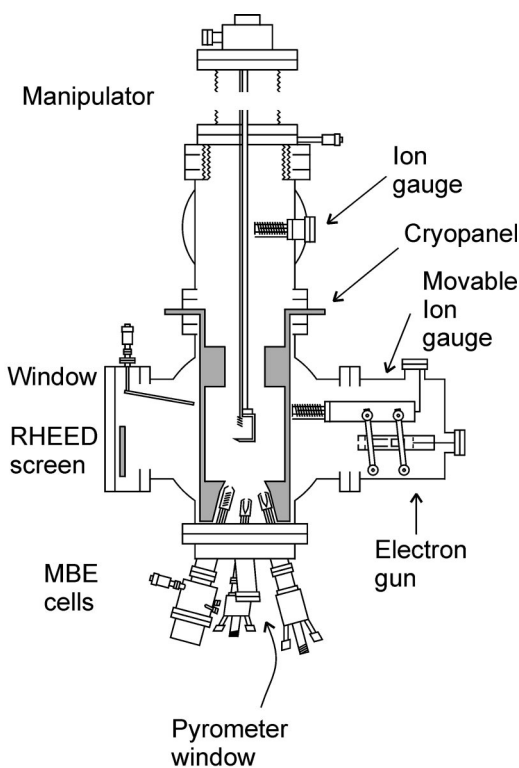


FIG. 2. Side view of the compact molecular beam epitaxy growth chamber.

tron gun mounted on two parallel swivel arms. The one at the backside is at the bottom attached to a rotary feedthrough. By turning the feedthrough, the ion gauge is moved into the center of the chamber, which corresponds in Fig. 2 to a movement from the right- to the left-hand side.

The chamber has a base pressure of 1×10^{-10} mbar achieved with an ion-getter pump (MECA 2000, PID 200, 200 l s^{-1}) and a Ti sublimation pump (Balzers, USP 034). In addition, there are cryopanel installed, which are filled with liquid nitrogen during MBE growth to keep the background pressure below 5×10^{-9} mbar.

B. Analysis chamber

The surface analysis chamber houses a low-energy electron diffraction (LEED) system (VSI, ErLEED) and a photoelectron spectrometer (VG, ADES400). Angle-resolved photoemission experiments are performed in the laboratory using a helium discharge lamp or at the toroidal grating monochromator 4 beamline of BESSY I. In addition, there are a 0.5–2 keV sputtering ion gun for sample cleaning and a mass spectrometer. The latter is used for leak checking in the entire system after bakeout. A pressure below 5×10^{-11} mbar is established in this chamber by a magnetically suspended turbomolecular pump (Balzers, TPU 180, 170 l s^{-1}).

C. STM chamber

The scanning probe microscope is mounted in a small chamber with a $\varnothing 140$ mm view port on top in order to have free vision towards the STM. The chamber is pumped by an ion-getter pump (Varian, Noble Diode, 135 l s^{-1}) which provides a base pressure of 1×10^{-10} mbar. The UHV-STM/AFM (atomic force microscope) was manufactured by Park Scientific Instruments (Autoprobe VP2). We have chosen this apparatus for several reasons. First, all movements, i.e., both coarse approach and fine motion, are performed at the scanner side. Thus the sample stage is freely accessible without complicated transfer mechanisms. Second, the instrument is able to load our heavy (55 g) tantalum sample carrier. The vibration isolation in this STM is achieved by a two-stage coil-spring suspension with eddy current dampers. Only a new set of adequate coil springs was required to support the sample carrier and fulfill the vibration isolation. The weight of the sample carrier makes, on the other hand, an additional fixing of the sample unnecessary. It is held just by its own weight on a U-shaped stainless steel holder, which is insulated against the sample stage. A disadvantage of the microscope as delivered by the manufacturer is that there is no possibility to insert new tips, without breaking the vacuum. Although there is a tip storage facility for six tip holders, a tip transfer mechanism out of the chamber is desirable. This is especially the case, if both AFM and STM tips are in use. Since STM tip contamination occurs quite often when measuring GaAs, the application of the STM is limited by the lifetime of the tips that are available. Hence, we have constructed a tip transfer, which will be described below.

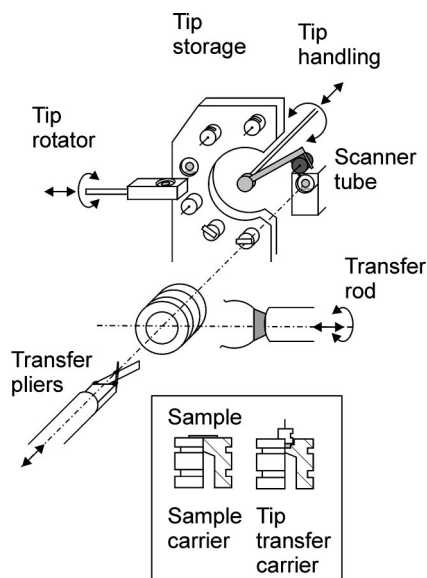


FIG. 3. Perspective sketch of the sample and tip handling. The inset shows the sample and the tip transfer carrier in half cutaway view.

D. Sample handling

1. Sample holder

The main difficulty of *in situ* investigations is the sample transfer between the different chambers. The key component of our sample transfer system is the cylindrical carrier made of Ta, shown in a half-cutaway view in the inset of Fig. 3. GaAs samples with typical dimensions $10\text{ mm} \times 10\text{ mm} \times 0.5\text{ mm}$ are fixed onto it with indium. To mount the sample carrier onto the manipulators and onto the transfer rod with its fork-like grips two 2 mm deep grooves are milled into the outside. On the backside there is a hole which accepts the transfer pliers of the transfer to the STM chamber. Furthermore, during MBE growth the heating filament is inserted into this hole so that effective heating by radiation is achieved. This way fast changes of sample temperature are possible.

2. Transfer lines

The transfer between the MBE and the analysis chamber is performed by a 1.4 m long magnetically coupled linear-rotary transfer rod (Huntington, VFC-169-36). It is driven by two direct-current motors, allowing precise and fast sample movement. Moreover, the motors are remote controlled and thus the transfer can be operated by only one person. After growth the samples can be moved out of the growth chamber within 20 s and afterwards cooled down to room temperature in another chamber. This can be important in cases where the desired surface reconstruction is cation rich, and further As adsorption on the surface has to be prevented.

The transfer line to the STM chamber is operated perpendicularly to the transfer line between the MBE and the analysis chamber (see Fig. 1). This transfer is also motorized and there is a pair of inverted pliers at the end of the transfer rod which fits into the hole of the sample carrier, as shown in Fig. 3.

E. STM-tip handling

1. Tip transfer

The tip handling available in the microscope, sketched in the upper part of Fig. 3, consists of a linear-rotary drive with an L-shaped arm at the end. This is inserted in the slot of the tip holder which is then clamped by a clip spring. With the linear-rotary motion tips can be moved from the storage to the scanner tube, where they are attached magnetically, and vice versa, as depicted in Fig. 3. In order to transfer the tip holder out of the chamber, we have installed a tip rotator, i.e., a second linear-rotary drive perpendicular to the tip holder handling arm. Here, a 1 mm deep hollow with a small magnet in its center is present, identical to those of the tip storage. A tip holder can be taken over and rotated by 180° , as indicated in Fig. 3. Tip transfer is performed by positioning the hollow on the tip rotator in the range of the tip handling arm, the tip holder is then placed in it, where it is attached magnetically. Afterwards the tip holder is rotated by 180° and taken over again from the tip handling arm. The tip is now directed towards the scanner position, where it is adopted by a specially designed cylindrical carrier similar to the sample carrier, as depicted in the cutaway view in the inset of Fig. 3. The tip carrier has a hollow in the front face where the tip holder can be attached magnetically. The tip carrier fits to the further transfer line, so that the tip carrier can be transferred via the loading chamber of the vacuum chamber.

2. Tip preparation

Our STM tips are either clipped or etched from tungsten wire. While clipped tips can often be used in UHV without further preparation, etched tips are often covered with oxides after the etching process. These oxides cause unstable tunnel currents. Therefore, tips have to be prepared further in vacuum. There are several methods employed to clean the tips and improve the tip quality. We use two different methods.

In the first one, the tip handling linear-rotary feedthrough line is used to position the tip in front of a filament. While the tip is connected to ground via the linear-rotary feedthrough, the filament is biased negatively. Electrons flow towards the tip and heat it, yielding the sublimation of the WO_3 .⁵ The removal of the oxide layer is indicated by an increase of pressure. Although this annealing method is easy to employ a big disadvantage exists, since there is no possibility to exactly determine when the process has to be stopped. This is a very important point, because the heating of the tip often ends in melting its apex and the tip loses its sharpness. However, carefully employing this procedure provides good tips and can also be used when the tip is contaminated by arsenic.

The second *in situ* tip preparation method, specially suited for etched W tips, employs field emission.⁶ A (111) orientated Au crystal is positioned on the sample stage and biased with -300 V while the tip is grounded. The tip is then moved close to the crystal until field emission occurs. It is believed that a rearrangement of atoms or desorption of foreign material from the tip apex are induced by the field emis-

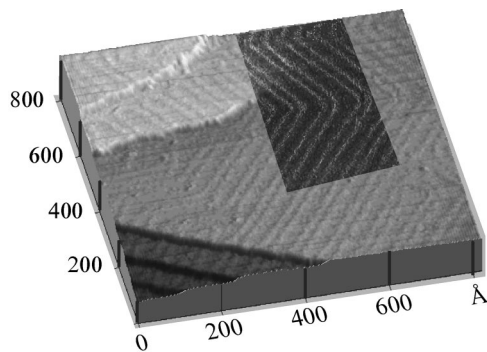


FIG. 4. STM image of the reconstructed Au(111) surface ($800 \text{ \AA} \times 800 \text{ \AA}$, -0.5 V , 0.2 nA). A large terrace showing the herringbone pattern (highlighted in the inset) as well as three steps on the lower left-hand side of the image can be seen. The step height is 2.3 \AA . On the upper left-hand side of the image the formation of two screw dislocations are visible.

sion with increasing emission current.⁷ The tip is moved closer to the sample and/or the applied voltage is increased until a breakdown of the emission current occurs. This breakdown is assigned to a decapitation of the tip, and a clean and sharp tip remains. The applied voltage is then immediately turned off and the tip is retracted.

An important advantage of the Au tip preparation technique is that the tip quality can be checked immediately by imaging the Au surface. A typical image of the Au surface is shown in Fig. 4 in a perspective view. One can clearly identify a large terrace with screw dislocations on the top and steps on the bottom part of the image. The step height of 2.3 \AA is in good agreement with the value known from literature.⁸ Moreover, imaging the $(22 \times \sqrt{3})$ reconstruction of the Au(111) surface is a very strong verification of the tip quality, since its corrugation is only 0.15 \AA .⁹ The corrugation is visible as the herringbone pattern highlighted with a different greyscale in Fig. 4 which arises from the accommodation of two extra atoms on the unit cell of the surface. The result is a mixed fcc and hcp atomic stacking on the topmost layer which appears as a herringbone pattern. The Au crystal is mounted on a standard sample carrier and is always kept under UHV conditions to avoid surface contamination.

III. RESULTS

A. GaAs(001)- $c(4 \times 4)$

To demonstrate the capability of the system for *in situ* semiconductor surface analysis, a STM image of the $c(4 \times 4)$ reconstruction of the GaAs(001) surface is shown in Fig. 5. The sample was grown in the MBE chamber under As rich conditions revealing the (2×4) reconstruction and hold under As flux at $450 \text{ }^\circ\text{C}$ for several minutes after growth. Then it was transferred to the analysis chamber, where it was cooled down to room temperature. The cooling is necessary in order to avoid drift in STM images due to thermal expansion of the scan piezo. The image was taken applying a sample voltage of -2.5 V and keeping the tunneling current at 0.3 nA (filled states). The brickwork-like nature of the reconstruction is clearly visible in the image. This structure is well known from literature and is caused by a dimerization of As atoms along $[110]$, while each ‘‘brick’’ is formed by

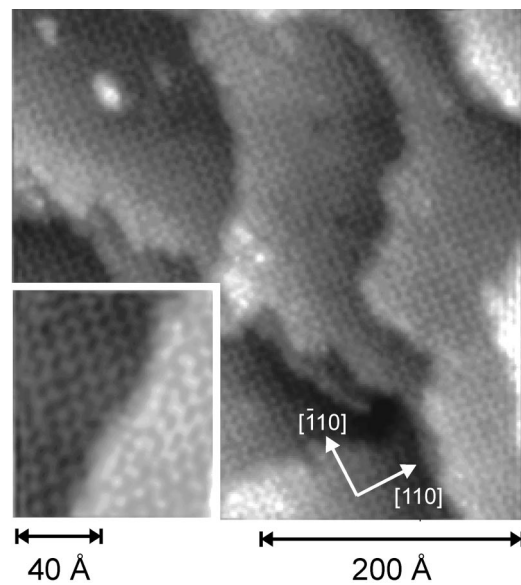


FIG. 5. Filled state (-2.5 V , 0.2 nA) image of the GaAs(001)- $c(4 \times 4)$ surface prepared by annealing at $450 \text{ }^\circ\text{C}$ under As flux after MBE growth ($800 \text{ \AA} \times 800 \text{ \AA}$).

three As dimers.¹⁰ Even though some terraces are present, which is caused by unintentional misorientation of the substrate, atomic resolution is obtained in the entire image. The surface is almost free of defects indicating a good quality of the sample preparation.

In summary, we have constructed a three chamber UHV system which is allowed to investigate *in situ* the growth of semiconductor surfaces at an atomic scale. Real space images are acquired with STM.^{11,12} Data on the surface reconstruction and on the crystallographic quality can be extracted from electron diffraction experiments (RHEED and LEED) yielding images in reciprocal space.¹³ Studies on the electronic structure, i.e., the chemical bonding, of the surface by photoemission are possible.¹⁴ The system enables us to investigate MBE grown layers *in situ* and thereby to contribute to the fundamental understanding of surface reconstructions and growth mechanisms of III/V semiconductor surfaces.

ACKNOWLEDGMENTS

The authors thank Professor G. Ertl for support. The project was also supported by the Deutsche Forschungsgemeinschaft (Sonderforschungsbereich 296) and by the German Bundesministerium für Bildung und Forschung under Grant No. 05622 EBA4.

¹D. Leonard, M. Krishnamurthy, C. M. Reeves, S. P. Denbaars, and P. M. Petroff, *Appl. Phys. Lett.* **63**, 3203 (1993).

²D. J. Eaglesham and M. Cerullo, *Phys. Rev. Lett.* **64**, 1943 (1990).

³B. Daudin, F. Widmann, G. Feuillet, Y. Samson, M. Arlery, and J. L. Rouvière, *Phys. Rev. B* **56**, R7069 (1997).

⁴D. Bimberg, M. Grundmann, and N. N. Ledentsov, *Quantum Dot Heterostructures* (Wiley, Chichester, 1999).

⁵C. J. Chen, *Introduction to Scanning Tunneling Microscopy* (Oxford University Press, New York, 1993).

⁶J. Wintterlin, Ph.D. thesis, Freie Universität Berlin, 1988.

⁷J. A. Meyer, S. J. Stranick, J. B. Wang, and P. S. Weiss, *Ultramicroscopy* **42–44**, 1538 (1991).

- ⁸D. D. Chambliss and R. J. Wilson, *J. Vac. Sci. Technol. B* **9**, 928 (1991).
- ⁹U. Harten, A. M. Lahee, J. P. Toennies, and C. Wöll, *Phys. Rev. Lett.* **54**, 2619 (1985).
- ¹⁰A. R. Avery, D. M. Holmes, J. L. Sudijono, T. S. Jones, and B. A. Joyce, *Surf. Sci.* **323**, 91 (1995).
- ¹¹L. Geelhaar, J. Márquez, K. Jacobi, A. Kley, P. Ruggerone, and M. Scheffler, *Microelectron. J.* **30**, 393 (1999).
- ¹²K. Jacobi, J. Platen, C. Setzer, J. Márquez, L. Geelhaar, C. Meyne, W. Richter, A. Kley, P. Ruggerone, and M. Scheffler, *Surf. Sci.* **439**, 59 (1999).
- ¹³C. Setzer, J. Platen, H. Bludau, M. Gierer, H. Over, and K. Jacobi, *Surf. Sci.* **402–404**, 782 (1998).
- ¹⁴J. Platen, C. Setzer, W. Ranke, and K. Jacobi, *Appl. Surf. Sci.* **123/124**, 43 (1998).